DESCRIPTIVE ARTICLE

ASE

The Development of a Virtual 3D Model of the Renal Corpuscle From Serial Histological Sections for E-Learning Environments

Jeremy A. Roth,[1] Timothy D. Wilson,[2,3] Martin Sandig[2,3]*

[1]*Department of Kinesiology, Faculty of Applied Health Sciences, University of Waterloo, Waterloo, Ontario, Canada*

[2]*Department of Anatomy and Cell Biology, Schulich School of Medicine and Dentistry, Western University, London, Ontario, Canada*

[3]*Corps for Research of Instructional and Perceptual Technologies (CRIPT), Schulich School of Medicine and Dentistry, Western University, London, Ontario, Canada*

Histology is a core subject in the anatomical sciences where learners are challenged to interpret two-dimensional (2D) information (gained from histological sections) to extrapolate and understand the three-dimensional (3D) morphology of cells, tissues, and organs. In gross anatomical education 3D models and learning tools have been associated with improved learning outcomes, but similar tools have not been created for histology education to visualize complex cellular structure–function relationships. This study outlines steps in creating a virtual 3D model of the renal corpuscle from serial, semi-thin, histological sections obtained from epoxy resin-embedded kidney tissue. The virtual renal corpuscle model was generated by digital segmentation to identify: Bowman's capsule, nuclei of epithelial cells in the parietal capsule, afferent arteriole, efferent arteriole, proximal convoluted tubule, distal convoluted tubule, glomerular capillaries, podocyte nuclei, nuclei of extraglomerular mesangial cells, nuclei of epithelial cells of the macula densa in the distal convoluted tubule. In addition to the imported images of the original sections the software generates, and allows for visualization of, images of virtual sections generated in any desired orientation, thus serving as a "virtual microtome". These sections can be viewed separately or with the 3D model in transparency. This approach allows for the development of interactive e-learning tools designed to enhance histology education of microscopic structures with complex cellular interrelationships. Future studies will focus on testing the efficacy of interactive virtual 3D models for histology education. Anat Sci Educ 8: 574–583. © 2015 American Association of Anatomists.

Key words: histology education; microscopic anatomy education; undergraduate education; three-dimensional model; renal corpuscle; kidney structure; visualization; 3D reconstruction; segmentation; serial sections

INTRODUCTION

Since early years in the millennium, the field of gross anatomical education has witnessed a substantial increase in the use of virtual three-dimensional (3D) models (Trelease et al., 2008). As interest in these models and related computer-assisted instruction (CAI) programs grows, so does the debate in the literature over their value and efficacy (Tam, 2010). Four out of eight studies concluded that the use of CAI improved the knowledge of the subject matter, when compared to traditional modes of learning (e.g., text and

*Correspondence to: Dr. Martin Sandig, Department of Anatomy and Cell Biology Western University London, Ontario N6A 5C1, Canada. E-mail: martin.sandig@schulich.uwo.ca

Received 3 October 2014; Revised 23 February 2015; Accepted 25 February 2015.

Published online 23 March 2015 in Wiley Online Library (wileyonlinelibrary.com). DOI 10.1002/ase.1529

2D images) (Hallgren et al., 2002; Elizondo-Omaña et al., 2004; Qayumi et al., 2004; Nicholson et al., 2006). Although the results regarding the efficacy of 3D models and related CAI have not formed a consensus, the literature is far more congruent with respect to student perception of such CAIs. The majority of studies investigating 3D visualization and CAI for the anatomy education report positive perceptions and high satisfaction when using the learning tools, compared to traditional learning methods (Silén et al., 2008; Petersson et al., 2009; Venail et al., 2010; Codd et al., 2011; Keedy et al., 2011). It is unclear how much of one's positive perception is related to the novelty of the medium, rather than the true perceived usefulness of the tool. Nevertheless, if designed correctly, a distinct advantage of virtual 3D models is that it can provide not only the key spatial information that is provided in a prosection, but also the clear and relevant information that one finds in a textbook (Codd et al., 2011).

Histology is the study of the normal microscopic anatomy of cells, tissues and organs. Within the anatomical and medical sciences, histology is an essential component in understanding normal and pathological structure–function relationships, yet the subject is often difficult to learn and to teach. An important technological advancement in histology education was the advent of virtual microscopy (VM) in which histological sections on glass slides are digitized and made available online (Drake et al., 2009). Conventional light microscopy (LM) is quickly being replaced by VM in North American classrooms and teaching laboratories and is well suited for distance learning programs. Indeed, a survey of medical schools in the United States found that the percentage of schools using only VM in their histology course increased from 14% in 2002 to 44% in 2009 (Drake et al., 2009). Both students (Harris et al., 2001; Braun et al., 2008; Husmann et al., 2009; Higazi, 2011; Helle et al., 2013) and educators (Husmann et al., 2009; Collier et al., 2012; Barbeau et al., 2013) have responded positively to the rising use of VM in histology. These digital learning resources provide some distinct advantages. Firstly, the sections can be annotated, viewed and studied outside of class or laboratory time. With many classes now being offered via distance education, VM technology is integral for offering consistent histology instruction for each student in all locations (Pinder et al., 2008). Secondly, with VM multiple students can simultaneously view the same slide, increasing possible collaboration and teamwork (Braun et al., 2008). Team-based approaches in VM, in fact, have been associated with improved examination scores in histology courses (Goldberg et al., 2007). Thirdly, students are increasingly more comfortable with using computers and accessing the internet than learning to use a LM (Harris et al., 2001). By using digital histology resources, educators can reduce unnecessary cognitive load, freeing more cognitive resources for learning the relevant histological information (Husmann et al., 2009). This advantage, however, is no longer applicable if the VM interface is poorly designed, thereby possibly increasing the cognitive load of the user (Wilson, 2015). Lastly, students generally feel that using VM is a more efficient use of their time than LM (Harris et al., 2001). The positive effect that VM has had on histology education indicates that there is potential for further integration of other novel computer-based learning environments in histology curricula.

Students of histology view two-dimensional (2D) sections taken through tissues, and are challenged to conceptualize the 3D structure of the tissue. This may lead to misinterpretations of the spatial relationships between various structures. Moreover, structural components that are important for visualization and understanding of the tissue may not be present in a particular 2D section. This lack of information can lead to conceptual inaccuracies and misleading interpretations of cellular and tissue function in relation to their structure. To overcome this problem many texts of histology therefore present to the learner 3D diagrammatic illustrations of tissues and organs side by side with histological sections. These illustration, however, are often artists' conceptions that oversimplify the 3D morphology of a tissue and learners often struggle with connecting the illustrations with what they see in the 2D histological section. The idea of creating 3D representations of histological structures using serial histological sections is not an entirely new one (Blumer et al., 2002; Ruthensteiner, 2008; Handschuh et al., 2010; Ruthensteiner et al., 2010). Specifically for tissues with complex cellular architecture, such as the kidney, 3D reconstructions were attempted since the 1970s (Ware, 1975). Using serial sectioning and LM, combined with various computer software algorithms, the 3D organization of entire mouse (Zhai et al., 2006) and rat (Christensen et al., 2014) nephrons was examined to elucidate renal transport mechanism. At the ultrastructural level the glomerular mesangium (Cho et al., 1991; Inkyo-Hayasaka et al., 1996), the glomerular capillary network (Remuzzi et al, 1992) and the podocyte architecture (Neal et al., 2005) were analyzed by 3D reconstruction. Most of the previous work, however, focused on applying this technique to measure and understand physiological parameters, rather than for education purposes of teaching mammalian histology in the medical or science undergraduate curriculum.

One major reason that hindered the use of 3D reconstruction in teaching histology is the labor-intensive necessity of generating vast amounts of serial sections to visualize entire tissues, and having to segment specific structures of interest for 3D rendering. More recently, however, Handschuh et al. described a method for creating 3D visualizations of vertebrate and invertebrate specimens that maintain the "true" stain color in the serial sections through the volume rendering segmentation method (Handschuh et al., 2010). The 3D visualization was highly detailed, but was meant for research in developmental biology and not for histology education (Handschuh et al., 2010). Likewise, Ruthensteiner published a highly detailed methodological paper on 3D visualization of specimens for morphological analysis, without discussing the possible advantages for core histology education (Ruthensteiner, 2008). Because these digital 3D models are not intended for wide distribution and student utilization, as seen with virtual slide boxes, they often remain in proprietary programs that are not accessible (both in price and usability) to the average student or educator. Furthermore, often little care is given to the aesthetics, interactivity, or level of user expertise of the 3D model. For the stated purpose of research, those 3D models prove adequate; however, virtual 3D models used for learning environments must not only be histologically accurate but also should be visually pleasing such that learners would be inclined to engage with the material.

The production of serial histological sections for LM is a straightforward technique in pathology laboratories. Here, tissue is normally embedded in paraffin, the sections are usually 10μm thick, and then stained with histological stains or

labeled with antibodies. This process is highly automated and can generate vast amounts of serial sections with little involvement of human labor. The morphological integrity of paraffin-embedded tissue, that lends itself well for serial sectioning with regular microtomes, is often inadequate for high-resolution imaging required for 3D visualization. In contrast, the embedding of tissue in epoxy resin compounds, which is mostly used for electron microscopy, ensures superior morphological integrity without distortions, and allows section thickness to be reduced to below 1 μm resulting in higher spatial resolution for 3D reconstruction. However, the production of serial sections from plastic embedded tissue is not routine, requiring special microtomes, glass or diamond knives, and is labor intensive. It is therefore not surprising that 3D imaging in histology education has lagged behind the advances in 3D imaging in the field of gross anatomical education. To overcome this shortcoming a virtual 3D model of the renal corpuscle was generated based on serial semi-thin epoxy resin sections that allows for an interactive and seamless combinatory view between 2D histological section and 3D morphology. It is hypothesized that such an approach in the study of histology will help bridge the cognitive gap between the 2D and 3D in undergraduate histology education. Currently, there is a paucity of research directed towards the design and effective testing of such histological models and this work represents first steps in that direction.

THE VIRTUAL THREE-DIMENSIONAL (3D) MODEL OF THE RAT RENAL CORPUSCLE

Specimen Processing for Histology

To generate an accurate virtual 3D model of the renal corpuscle at a high level of resolution, epoxy resin (Epon/Araldite) embedding of kidney tissue was used to produce complete ribbons of serial semi-thin (1μm thick) sections. Rat (Sprague/Dawley) kidneys were fixed by perfusion in 4% formaldehyde. The cortex of a kidney was then cut into approximately 9 mm^3 cubes and fixed overnight in Karnovsky's fixative (Karnovsky, 1965) with one change of fixative. The tissue was dehydrated in increasing concentrations of ethanol, followed by infiltration with 100% propylene oxide. The tissue was drained of the propylene oxide and placed for 1 hour in a 1:1 mixture of propylene oxide and the embedding medium consisting of 5 mL Embed-812, 3 mL Araldite, 11 mL DDSA, and 0.3 mL DMP-30 (Mollenhauer, 1964). The tissue was then infiltrated overnight with 100% embedding medium. Fresh 100% embedding medium was added to the tissue and mixed for 3 hours. Tissue specimens were then embedded in fresh medium and degassed under vacuum. Polymerization occurred for approximately 72 hours at 60°C. Trimming of the specimen block occurred under a stereomicroscope with a one-sided razor blade. The block face and resultant sections had a trapezoid shape and measured approximately 2 mm × 2 mm in size with parallel upper and lower edges to ensure strait ribbons (Blumer et al., 2002; Ruthensteiner, 2008). To produce ribbons of serial sections, the sections must stick together. This was achieved by applying the adhesive Pattex Compact (Henkel KGaA, Düsseldorf, Germany) to the lower block face at a dilution of six drops of xylene to 5 mm^3 volume of adhesive (Henry, 1977; Ruthensteiner, 2008). The adhesive Weldwood Contact Cement

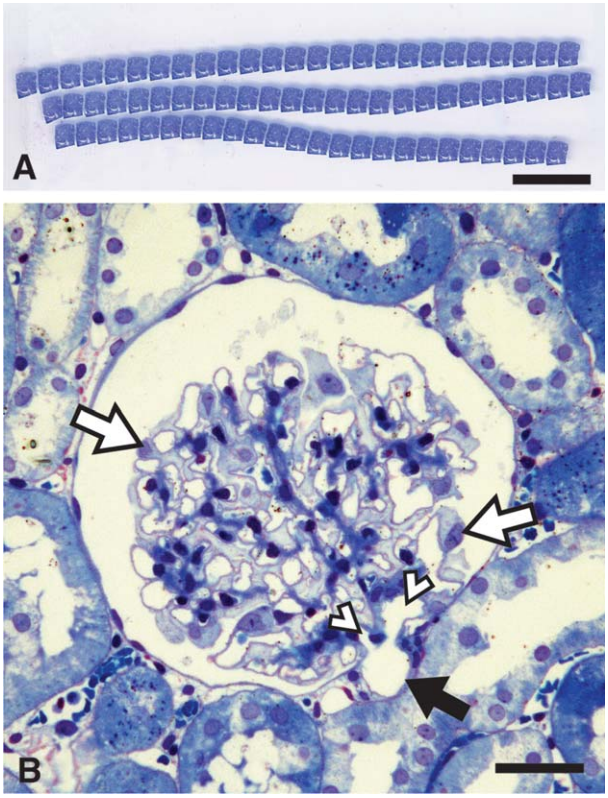

Figure 1.

Stained histological sections. (**A**) Three ribbons of stained sections (~25 each) generated with the histo jumbo diamond knife and mounted on a microscope slide; (**B**) High magnification micrograph showing one of three renal corpuscles present in most of the histological sections. This section is about midway through a complete series of sections through a renal corpuscle used to create the virtual 3D model. Clearly distinguishable are the afferent arteriole (black arrow) ramifying into two branches of glomerular capillaries (arrowheads), and podocyte nuclei (white arrows). Bar in panel A = 1 cm, in panel B = 50 μm.

(DAP Products, Baltimore, MD) is also suitable for this purpose (Ruthensteiner, 2008). The tissue was sectioned with an Ultracut E ultramicrotome (Reichert Inc., Depew, NY) into semi-thin sections, 1 μm in thickness, using a histo jumbo diamond knife (Diatome AG, Biel, Switzerland) (Blumer et al., 2002; Ruthensteiner, 2008). The large trough available on this diamond knife, when filled with water, allowed for several long ribbons to be sectioned and accommodated on one slide. Approximately three ribbons at a time were picked up onto microscope slides (Fig. 1A) that were cleaned and pretreated with an ethanol (96%) ammonia (25%) solution at a ratio of 9:1 to reduce surface tension and facilitate adherence of ribbons to the glass surface (Ruthensteiner, 2008). This was done by sliding a slide underneath the ribbons at an angle, allowing one end of the ribbons to contact the slide. When lifting the slide out of the water ribbons then floated on a large water drop on top of the slide. Five slides were produced with three ribbons of approximately 25 sections each for a total of 375 sections. It was necessary to produce this large number of sections to increase the likelihood of capturing an entire renal corpuscle within the sample of serial sections. The slides were placed on a hotplate for 1 hour

at 60°C to allow for the stretching and firm adherence of sections onto the glass surface. After all of the water had been evaporated sections were stained with methylene blue azure B (MBAB) and basic fuchsine (BF), (D'Amico, 2005). MBAB was added to the slide first to sufficiently cover the ribbons and left on the hot plate for five minutes at 60°C. The stain was rinsed off with distilled water, taking care not to directly disturbing the ribbons. BF was added to the slide subsequently for 1 minute at 60°C, and sections were once again rinsed with distilled water and dried. These two stains allowed for distinguishing substructures within the sections in high detail. Nuclei appeared dark blue to light purple depending on the cell type (Fig. 1B, white arrows), while basement membranes were stained reddish-violet. Tissue and cellular integrity was maintained to a high degree by the fixation and embedding protocol used. Indeed, the basement membrane of the capillaries was readily visualized, which was essential when segmenting the glomerular capillary lumina. These vessels and their branching patterns were readily discernable (Fig. 1B, black arrow, white arrowheads). Of the total 375 sections generated, 179 contained the renal corpuscle used for building the model and were digitally photographed and archived.

Digital Microphotography and Image Pre-treatment

A Leica DM2000 microscope equipped with a Leica DFC 425 digital camera (Leica Microsystems, Wetzlar, Germany) and a 40× objective were used to photograph a renal corpuscle throughout consecutive sections. The exposure, saturation, and gain of each photograph were adjusted in the Leica LAS software (Leica Microsystems, Wetzlar, Germany) to ensure that each photograph would have similar contrast, brightness, and color values. The images were cropped and converted to grayscale using the batch function in Adobe Photoshop CS3 (Adobe Systems, San Jose, CA). Both the original RGB color and grayscale copies of the images were saved. The grayscale images were used for creating the virtual 3D model, whereas, the RGB color images were used for reference.

Creation of a Virtual 3D Renal Corpuscle

Incorporating techniques previously described for gross anatomical virtual model creation (Hu et al., 2009; Nguyen et al., 2009; Sergovich et al., 2010; Adams et al., 2011; Yeung et al., 2011), the grayscale images were imported into the 3D software, Amira 5.2 (Mercury Computer System, Chelmsford, MA) as an image stack in the XY axis. Within the image stack, each image is known as a slice. To calibrate the X, Y, and Z dimensions in the *crop editor* to the correct voxel size (a volumetric pixel with the added dimension of depth) for the 3D model, the Z dimension was set to 1 μm, the thickness of the section. To calculate the X and Y dimensions, an ocular and stage micrometer was used to measure the length and width of a pixel, which equaled 0.226 μm. For a detailed protocol on calibrating the X, Y, and Z dimension, see Section 2.5 Amira-import—calibration in the paper published by Ruthensteiner (2008). Since it was not possible to photograph the renal corpuscle in the exact same orientation in each section, the *alignslices* tool was used to align the images in the images stack (Ruthensteiner, 2008). Manual segmentation was used to create 3D models of structures of interest within the renal corpuscle. Segmentation is the manual process of selecting a region of interest (ROI) from an image and assigning it to a label (Tam, 2010). In the *Segmentation Editor* of Amira the *paint brush* tool was used to manually select ROIs in each slice of the image stack. The image data were viewed within the *Segmentation Editor* in the three orthogonal axes (XY, XZ, and YZ) and, thus, the images in all three axes were used for segmentation. For certain structures that do not significantly change shape or position from one section to another (i.e. arterioles or tubules) an interpolation technique was used. Interpolation is a semi-automated tool in Amira, which applies a predictive algorithm to select voxels between two manually segmented slices. To interpolate, the *paint brush* tool was first used to select the ROI in every third slice. The interpolation algorithm was then used to select the appropriate voxels in the intervening slices. Selected voxels were assigned to a label, known as a *Material*, and a separate *Material* was created for each structure of interest in the renal corpuscle. A representation of the Amira *Segmentation Editor* interface is shown in Figure 2. The ability to view and segment the renal corpuscle in all three orthogonal axes was quite advantageous, since it permitted choosing the best axis for segmentation of a particular structure. For example, the afferent arteriole was oriented in a way in which segmenting in the XY axis was the best option, whereas the efferent arteriole was best segmented in the XZ axis. Furthermore, it was possible to localize the same point in 3D space on each axis by dragging the intersecting lines in one axis to the point of interest. This made it easier to confirm the identity of certain structures that were more difficult to identify (i.e., macula densa nuclei and nuclei at the transition from parietal cells to proximal convoluted tubule nuclei).

Although Amira is not an ideal program to launch a learning tool due to its expensive license, high computer processing requirements, and challenging interface (Martin et al., 2013), it does provide the user with the ability to view the 2D histological images in any plane within the context of the virtual 3D model. Once a stack of images, obtained from sections physically cut by a microtome in a particular orientation (Fig. 2A), is imported into Amira, the software readily generates images of virtual sections visualized at any chosen orientation (Figs. 2B and 2C). The software thus serves as a "virtual microtome" allowing 3D integration of the 2D information. This integration can be done in either the *Segmentation Editor* (Fig. 2), or by creating surfaces of each object using *SurfaceGen* module and then applying the *OrthoSlice* module to the original image data (Figs. 2E and 2F). The advantage of using the latter method is that the transparency of the surfaces is adjustable (Fig. 2F) enabling users to see through multiple layers. The user can scroll through the image stack in any plane and thus produce a virtual histological section at any orientation hence, the term "virtual microtome." An animation of the aforementioned capabilities is found at the laboratory's website (CRIPT, 2015).

The *SurfaceGen* module was applied separately for each segmented structure. The default number of faces for each structure was used and no smoothing was applied. The resulting new surface objects were saved as surface (.surf) files and exported from Amira as Wavefront object (.obj) files for further mesh surface modifications. Once all of the chosen structures were segmented, polygonal mesh surfaces of each structure were created in Amira. Each object was independently imported into the 3D mesh editing software, Mesh

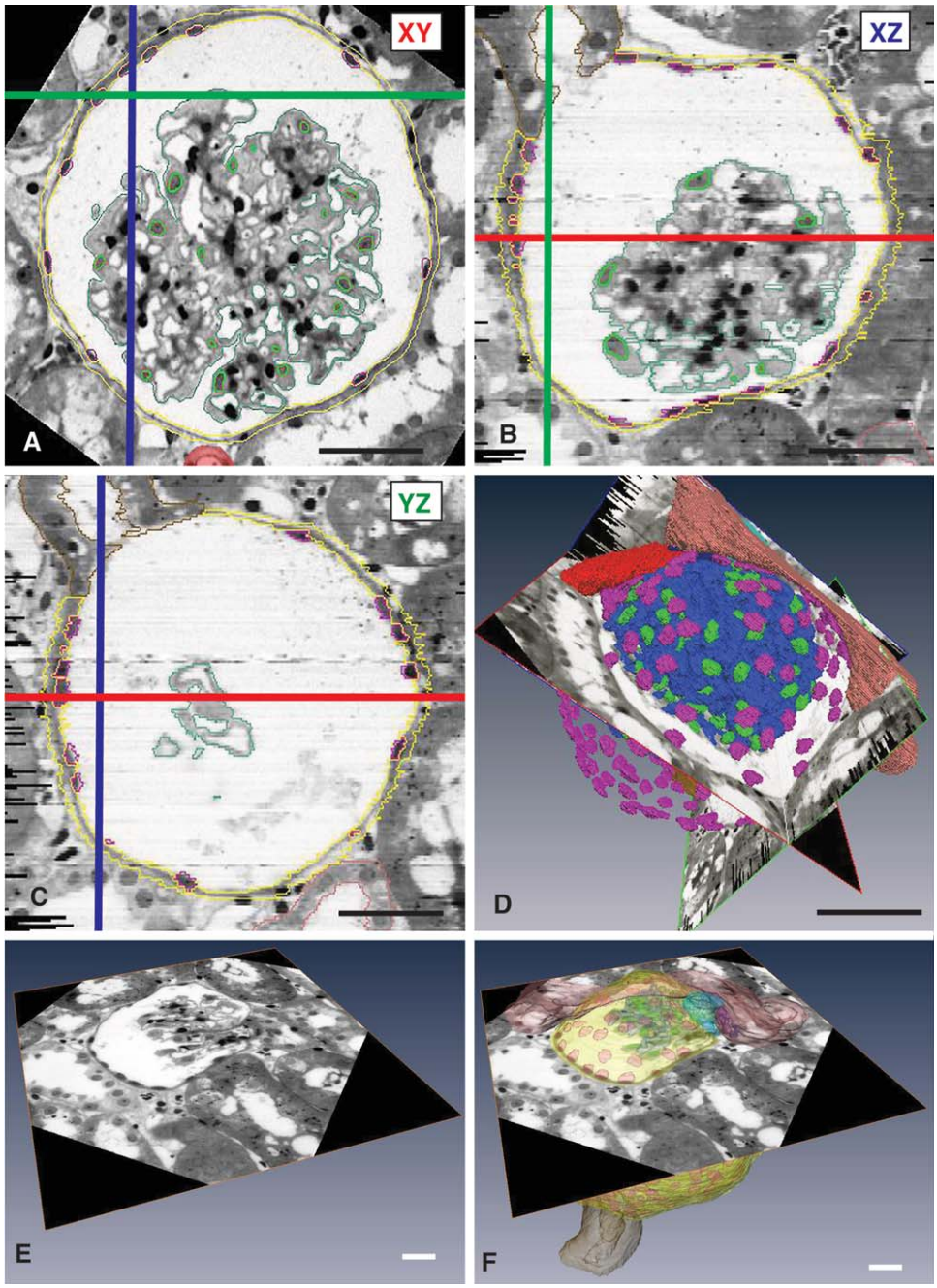

Figure 2.

Images captured from *Segmentation Editor* in Amira software. (**A**) Image of a section through the renal corpuscle from the original image stack in XY orientation; (**B**) Software-generated view in XZ orientation of a virtual section of the renal corpuscle taken along the blue line indicated in panel A; (**C**) Software-generated view in YZ orientation of a virtual section of the renal corpuscle taken along the green line indicated in panel A. The red line in panels B and C indicates the plane of the section shown in panel A. Also shown in panels A–C are manually segmented structures as thin outlines: yellow = Bowman's capsule, purple = nuclei of parietal capsule epithelium, green = podocyte nuclei, blue = glomerular capillaries, brown = proximal convoluted tubule, pink = distal convoluted tubule; (**D**) Combined view of 3D rendered structures within the renal corpuscle together with individual sections. The user can scroll through the real and virtual images to view the renal corpuscle at any section level and in any orientation; (**E**) *Orthoslice* in Amira: Image of a randomly selected section through the renal corpuscle showing part of Bowman's capsule, the glomerulus and surrounding distal and proximal convoluted tubules; (**F**) The user can add to the section the corresponding structures of the virtual 3D model of the renal corpuscle generated by manual segmentation. These appear as color-coded object surfaces and can be toggled on and off. Bar in panels A–D = 50 μm, in panels E and F = 25 μm.

Lab, version 1.2.1 (ISTI-CNR, Pisa, IT) (Allen et al., 2015). The object surfaces are represented as polygonal meshes, which are made up of many triangular faces. To reduce the number of faces in each mesh and, consequently, the file size of each object, the *Quadratic Edge Collapse Decimation* filter was applied. Each mesh remained unsmoothed and was exported from Mesh Lab as a Wavefront object (.obj) for further mesh processing.

Optimization of the Virtual Three-Dimensional (3D) Renal Corpuscle

The (obj.) files were imported into Blender 2.63 (Blender Foundation, Amsterdam, NL), an open-source 3D mesh editing software. It is important to note that the (.obj) files should be imported *together*, rather than *individually*, since this ensures that the objects remain in the proper orientation and location relative to each other. The object meshes were modified in *Edit Mode* to fix the issues of non-manifoldness. It is not uncommon for surface meshes exported from Amira to have multiple non-manifold issues; however, due to the convoluted shape of the glomerular capillaries and the thinness of the Bowman's capsule, an exceptionally high number of non-manifold issues had to be repaired. Once non-manifold errors were repaired, each mesh was smoothed to reduce their block-like appearance upon magnification. In Blender, smoothing was accomplished by adding a *Smooth* modifier to the object mesh, as well as changing the *Shading* from *Flat* to *Smooth*. The *Smooth* modifier in Blender was preferred over the *Laplacian Smooth* filter in Mesh Lab since the latter significantly altered the geometry of the meshes so that the object no longer fit together properly (e.g., the opening of the Bowman's capsule was larger than the proximal convoluted tubule). It also allows for easy previewing of the smoothed object in the context of the other objects. This ensured that the relative shape and size of the objects remained morphologically accurate. Smoothing the object meshes was an essential step for improving the appearance of the renal corpuscle model by reducing the block-like appearance. The *Shading* object tool in Blender was used to make an object appear smooth. Importantly, the *Smooth Shading* tool did not alter mesh geometry but changed how the 3D visualization program calculated shading on the surface. This tool proved to be a very useful compliment to the *Smooth* modifier, since certain objects could not be fully smoothed using the *Smooth* modifier without significantly altering the mesh geometry. Further manual modifications of the mesh were done in *Edit Mode* to ensure that all of the triangular faces in the object meshes faced the same direction. To do so, first the entire mesh was selected in *Edit Mode* and then, the *Recalculate* option under the *Normals* tool was chosen. It is also possible to manually choose the faces to be flipped by selecting the target face and choosing the *Flip Direction* option under the *Normals* tool.

Sharing the Virtual Three-Dimensional (3D) Renal Corpuscle Model

The objects were then exported from Blender separately as Wavefront (.obj) files and imported into the 3D game development program Unity 3.5.6 (Unity Technologies, San Francisco, CA). Unity has been found to be an excellent program for developing interactive learning tools (Allen et al., 2015). Although an interactive learning tool was not developed during this study, it was important to understand how the objects appeared in the new 3D environment to ascertain whether further mesh modification in Blender were necessary. For educational purposes, ten basic cellular/morphological structures were segmented and incorporated into the virtual renal corpuscle model (Fig. 3). These included: Bowman's capsule, nuclei of epithelial cells in the parietal capsule, afferent arteriole, efferent arteriole, proximal convoluted tubule, distal convoluted tubule, glomerular capillaries, podocyte nuclei, nuclei of extraglomerular mesangial cells, nuclei of epithelial cells of the macula densa in the distal convoluted tubule. When the 10 objects were initially imported into Unity from Blender it became apparent that the two programs differed in how shading was calculated. As a result, imperfections that were not easily seen in Blender became apparent in Unity. It was, therefore, necessary to make further modification of the mesh for most of the objects in *Edit Mode* in Blender to fix the imperfections. Once the additional modifications were finished, color was added to the meshes in Unity, using the *Create – Materials* tool under the *Assets* menu. The *Materials* were created by sampling the default color of each structure in Amira. The colors assigned to each structure were randomly assigned in Amira and can be changed in both Amira and Unity, if required. Figure 3 displays all ten of the renal corpuscle structures separately in Unity with the color *Materials* applied. Figure 4 shows the entire virtual 3D renal corpuscle model in Unity. When the Bowman's capsule and the distal convoluted tubule have been removed detailed internal structures, such as the podocyte nuclei, glomerular capillaries, and macula densa nuclei can be seen (Fig. 4B). This model is interactive in that it can be rotated in any desired orientation, select structures can be toggled on and off, and the individual histological images (from the original sections or virtually generated) can be displayed separately or in conjunction with the 3D model in any orientation.

DISCUSSION

This report outlines the steps necessary for creating morphologically accurate virtual 3D models of microscopic anatomical structure for use in E-learning environments. It became particularly evident that the generation of structurally accurate histological models depended most importantly on good quality images with high resolution derived from a complete set of semi-thin serial histological sections of epoxy resin-embedded tissue. Staining individual semi-thin sections of epon/araldite-embedded tissue is commonly used for evaluating the quality of tissues before use in transmission electron microscopy. However, it is not often used for routine light microscopic examination of tissues in histology and pathology. Embedding in epoxy resins, as opposed to the commonly used paraffin wax, was preferred for two reasons. First, resin-embedded tissues maintain higher morphological integrity during sectioning; second, it is possible to generate significantly thinner sections due to the hardness of the polymerized resin. Since the generated histological images are stacked in Amira to create a 3D representation, resolution is defined in terms of voxels (volumetric pixels – pixels with depth) as opposed to 2D pixels. If X and Y are considered the width and height of an image, Z refers to the thickness of the image and, therefore, the section thickness. Ideally voxel dimensions are both small and isotropic indicating a cubic shape (X = Y = Z) (Handschuh et al., 2010) to avoid visual distortion. For two of the axes used during segmentation (XZ and YZ), the resolution of the images directly depends on the thickness of the image (Z). Since small structures identifiable with histological stains, such as nuclei, are often only 10 μm in diameter, they could be inaccurately segmented or completely lost altogether if the section thickness is too great. Hence, it was important to not only generate high-resolution images (X-Y dimensions), but also sufficiently thin sections

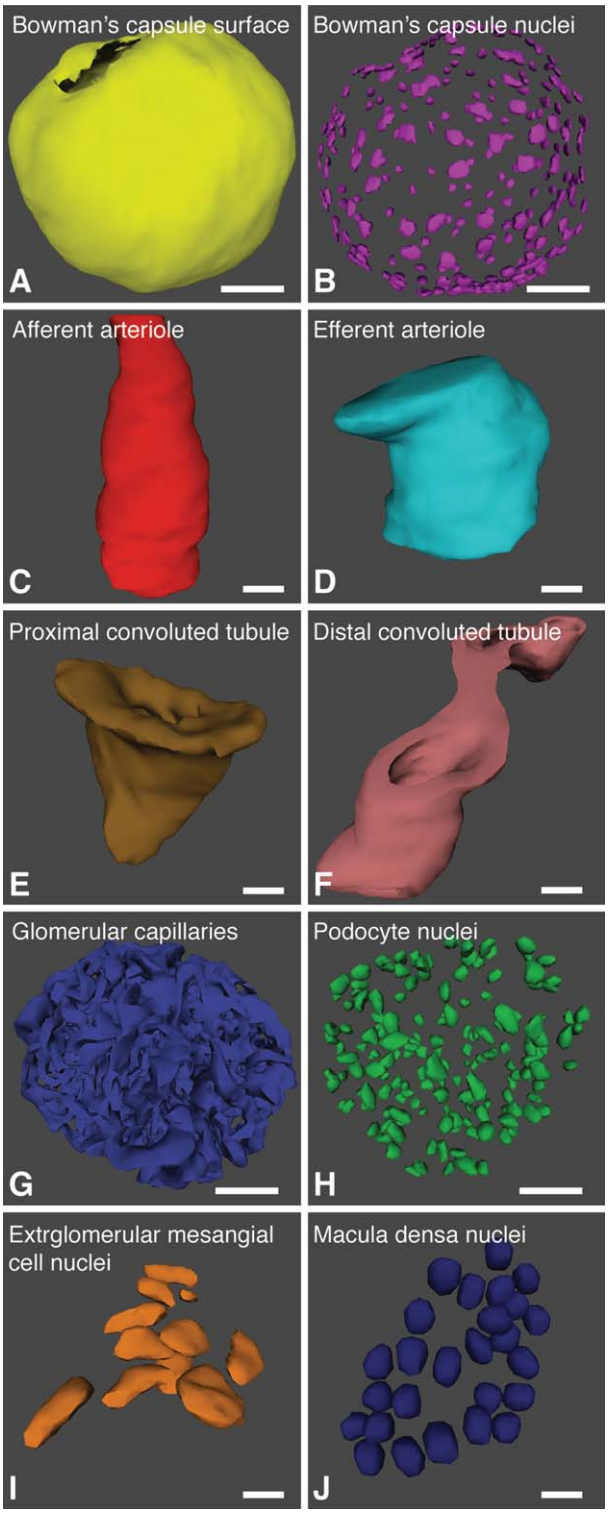

Figure 3.

The ten manually segmented structures of the virtual 3D renal corpuscle model in Unity software. (**A**) Bowman's capsule; (**B**) nuclei of epithelial cells in the parietal capsule; (**C**) afferent arteriole; (**D**) efferent arteriole; (**E**) proximal convoluted tubule; (**F**) distal convoluted tubule; (**G**) glomerular capillaries; (**H**) nuclei of podocyte; (**I**) nuclei of extraglomerular mesangial cells; (**J**) nuclei of epithelial cells of the macula densa in the distal convoluted tubule. Bar in panels A, B, G, H = 25 μm; in panels C, D, E, F, I, J = 10 μm.

(Z dimension) when creating virtual 3D models from histological sections.

The quality of the staining is another important factor when producing histological images that are sufficiently detailed for 3D reconstruction. The polychromatic staining method used distinguished podocyte nuclei from those of endothelial cells of the glomerular capillaries and the intraglomerular mesangial cells. In addition, BF stained the glomerular basement membranes distinct reddish-violet, which was particularly helpful when segmenting the lumen of the glomerular capillaries. Since the urinary space often intrudes between loops of glomerular capillaries it can be difficult to differentiate between urinary space and the lumen of a glomerular capillary within the glomerular tuft because they both appear white. The attenuated endothelial cells lining the lumen of the capillaries, and the overlying podocytes contribute both to the glomerular basement membrane, which was clearly visible as a reddish-violet line separating both cell types. It was, thus, possible to differentiate between urinary space and capillary lumen, because the urinary space had greyish blue podocyte cytoplasm between it and the reddish-violet basement membrane. The capillary lumen, on the other hand, was surrounded by and almost immediately adjacent to the basement membrane (with only the very thin endothelium separating the two). Without the detail provided by good fixation, intact morphology in thin sections, and the staining protocol, it would have been very difficult to differentiate between these structures within the renal corpuscle during segmentation.

There are several advantages to using real histological sections to create the virtual 3D model. Firstly, by reconstructing the 3D model of structures from a series of actual 2D sections, rather than based on an artistically perceived diagrammatic representation, the 3D morphology is rendered accurately and is unlikely to perpetuate possible false assumptions relating to morphology. Secondly, the images of the original sections along with sections created virtually, in the XZ and YZ planes, by the software (virtual microtome) can be integrated into the 3D learning tool, thereby allowing users to readily relate the 2D and 3D representations (Ruisoto et al., 2012).

Students typically learn histology by viewing 2D images and are challenged to infer 3D morphology and spatial relations within the structure. It was hypothesize that by viewing the 2D histological sections/images within the context of a corresponding morphological accurate 3D model, students will demonstrate improved understanding of the relevant morphology. It is conceivable that this training will help students to become more proficient in interpreting other 2D histological sections of similar or different structures. Since this is a novel approach within the field of histology education, little has been published on its pedagogical value. Previous studies have examined the effects of 3D representation of anatomical structures on students' ability to interpret 2D cross-sectional images, such as CT scans (Estevez et al., 2010; Metzler et al., 2012; Ruisoto et al., 2012). Metzler et al. investigated whether a 3D presentation of the Couinaud liver segments in a teaching module would improve student's understanding of the corresponding 2D CT scans (Metzler et al., 2012). The participants were divided into a 2D group, who were given a teaching module with only a series of consecutive transverse CT scans, and a 3D group, who were provided with the 2D teaching module with an accompanying 3D model based on the 2D scans. Two examinations were administered to both groups, with one week in between the

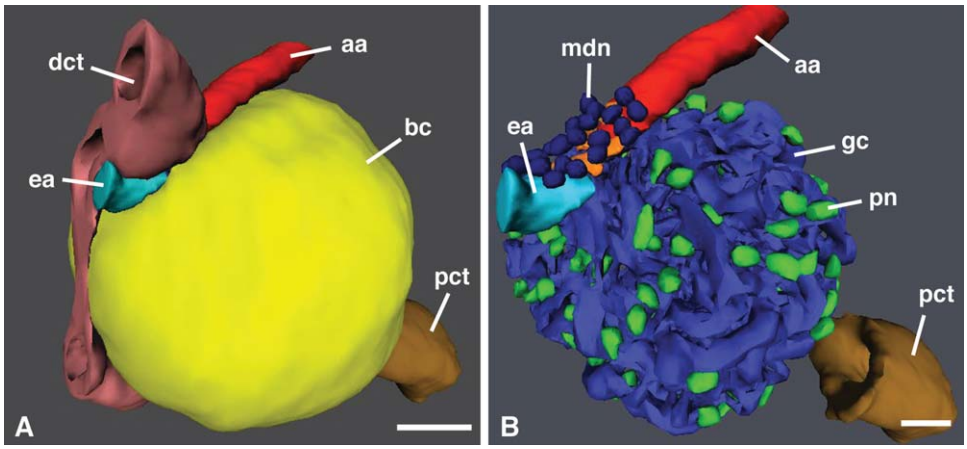

Figure 4.

Three-dimensional (3D) visualization of the entire virtual 3D model of the renal corpuscle. (**A**) The 3D model in *Unity* software showing Bowman's capsule (bc), as well as the location of the proximal (pct) and distal (dct) convoluted tubules and the afferent (aa) and efferent (ea) arterioles; (**B**) When Bowman's capsule and distal convoluted tubule are removed the relative location of the internal structures, such as nuclei of the macula densa (mdn), glomerular capillaries (gc), and podocyte nuclei (pn) become visible. Bar = 25 μm.

two examinations. Overall, there was no significant difference in examination scores between the 2D and 3D groups. For both groups, some of the participants withdrew from the study after the first examination. Interestingly, the participants from the 2D group who only finished the first examination performed significantly worse than the participants from the same group who finished the entire study. This phenomenon, however, was not observed for the 3D group. The authors hypothesized that learning with *only* 2D images may be more difficult than with the 3D visualization and, thus, increases the *initial* threshold for understanding the anatomy. For the 3D group, the two visualizations (2D and 3D) were not viewed together in the learning module, but rather, they were viewed separately on different areas of the screen. It is, therefore, unclear what the effect would be of viewing the 2D images (CT or histological sections) in the context of a corresponding 3D model.

Neuroanatomical education has constraints similar to those in histology education; both realms require interpretation of complex 3D structure recognition from seemingly ambiguous 2D images especially to the novice. Ruisoto et al. analyzed whether 3D visualization helps students locate and identify sub-cortical structures with more precision than 2D cross-sections (Ruisoto et al., 2012). Participants in the 3D visualization group were given a 3D model of the sub-cortical structure embedded in 2D cross-sections and asked to identify the structures. When compared to the 2D group, who only used 2D cross-sectional images to identify the structures, the 3D visualization group had higher success rates and confidence as well as decreased response time (Ruisoto et al., 2012). Furthermore, 3D visualization was better at facilitating the identification of particularly difficult structures. It is suggested that 3D visualization allows learners to form a more accurate representation of structures and the spatial relationship between them (Ruisoto et al., 2012). Since the learner does not need to create a mental 3D representation, more cognitive resources are available for learning the material of interest (Metzler et al., 2012, Chung et al., 2013). The virtual 3D model of the renal corpuscle model allows for incorporation of both the 2D histological images and the 3D model into an interactive learning tool. Such a tool may be particularly helpful for students when learning the 3D relationship of the key structures at a cellular level. Furthermore, students should be able to interpret the 2D histological images with improved accuracy and confidence (Ruisoto et al., 2012). Continued research is required to understand how virtual 3D models of histological structures, along with the 2D images, affects one's ability to both understand the structures involved as well as further interpret novel 2D sections of those structures. The generation of virtual 3D histology models may be a viable avenue to facilitate learning of difficult concepts and improve core histology education.

Surface rendering via manual segmentation is not the only method for creating 3D visualizations of histological or anatomical structures. Volume rendering, in which the contrast in color between different structures in the image stack is utilized to automatically render structures, has been used (Handschuh et al., 2010). Volume rendering does not, however, allow for toggling on and off specific structures, making it difficult to visualize structures deep within a model. More recently, a new technique known as CLARITY has been created (Chung et al., 2013). This technique permits the 3D visualization of cells without requiring physical sectioning of the tissue. Lipids are first removed from the tissue, causing the tissue to become nearly transparent and penetrable by macromolecules. Next, immunohistochemical markers are used to highlight different structures. Currently, the CLARITY technique has mostly been used in the field of neuroscience; however, the authors believe that the technique has the potential to be used in any organ system (Chung et al., 2013). Whether CLARITY will produce 3D visualization that will be useful for novice learners of histology remains to be seen. Since sectioning is not required, students will not have the original stained 2D histological images to refer to.

Limitations and Future Directions

Creating a model based on serial histological sections is a time-consuming endeavor that requires expertise in ultramicrotomy and some manual dexterity. In addition, surface rendering in Amira via manual segmentation is a lengthy process (Ruthensteiner, 2008). The total time for segmentation depends greatly on the number of structures chosen, the number of slices required, and whether the shape of the structure allows accurate interpolation. Since the efficacy of such 3D models in histology education has not been fully explored, it is difficult to assess whether further work to create more models is an effective use of an investigators resources.

Although semi-thin sectioning has greatly improved the level of resolution that was achieved for 3D modeling, 3D visualization of cellular and subcellular structures for educational purposes are subject to the resolving power of the light microscope. It was also not possible to segment individual cells, since junctions between cells are not visible with the general histological stains used. Specific cells of interest, such as parietal cells or podocytes, were only represented in the virtual 3D model as nuclei. It is possible that this could lead to certain misunderstandings for novice learners. For example, the Bowman's capsule is formed by parietal epithelial cells. In the current model, however, the surface of the Bowman's capsule and parietal cell nuclei were visualized as separate structures. This could lead to confusion for novice learners and must be addressed when designing an applicable learning tool.

Moreover, due to the limit of resolution it was not possible to reconstruct the relationship of the podocytes to the glomerular capillaries and how they fit together to form the important glomerular filtration barrier. The glomerular filtration barrier is viewed best using electron microscopy, in which the processes of the podocytes can be seen wrapping around the fenestrated capillaries with the glomerular basement membrane in between (Neal et al., 2005). Due to limitations in magnification and resolution, only the lumen of the glomerular capillaries and the podocyte nuclei were segmented. The podocyte nuclei are shown to reside on or within the glomerular tuft, but it was not possible to segment and visualize the cytoplasm and, the processes of the podocytes.

Without its incorporation into a digital learning tool, the virtual 3D model of the renal corpuscle is not overtly accessible to students of histology. Such a tool should incorporate the virtual 3D model along with the original 2D histological images. With such a learning tool at hand, several parameters could be tested regarding 3D visualization in histology such as: (1) effects of virtual 3D histological models on learning, (2) efficacy of the particular tool (i.e., does the learning tool produce equal or better learning outcomes than traditional teaching methods?), and (3) usability of the tool (i.e., is the tool easy to use? What are the barriers to effective usage?). The result of such studies will not only provide guidance to the difficult question of whether learning with virtual 3D models is appropriate for the context of histology education, but will also inform improved design of future learning tools. A particular phenomenon that warrants further research is the effect of viewing 2D images of a 3D structure in the context of a virtual 3D model of that 3D structure on one's ability to successfully interpret different or related 2D image. This question is an essential one for assessing the value of virtual 3D models in histology. There are currently very few papers investigating this phenomenon, all of which focus on learning gross anatomy for radiological image interpretation or neuroanatomy. Such a study would provide critical information for educators in the fields of histology and radiology education. Furthermore, it will be necessary to assess the educational level most appropriate for this model. The authors propose that it would be best used in an undergraduate level course as a supplementary tool when teaching renal histology. This could be done by making a virtual 3D model available online to the students and using such a tool for online quizzes and examinations. It is also feasible that the model could be used in medical education; however, the students in medical programs should acquire a higher level of understanding of the renal histology and physiology. An interactive virtual 3D teaching tool based on exact cellular morphology could be adapted to include modeling of blood flow and filtration rates in physiologically normal and pathological conditions.

CONCLUSIONS

In conclusion, the work presented here defines histological and technical steps required to build a virtual 3D histology model of the renal corpuscle. These steps involve generating serial semi-thin sections, the application of histological stains, and 3D reconstruction using Amira, Blender, and Unity softwares. The authors suggest that complementing pedagogic tools such as the one described here will be a valuable addition to virtual slide boxes for students of histology. It is being hypothesized that the interpretation of 2D views from histological slides can be augmented with a 3D overlay and virtual microtome capabilities to aid students' understanding of complex architecture of the kidney and other tissues.

ACKNOWLEDGMENTS

The authors thank Ms. Lauren Allen, M.Sc., Department of Anatomy and Cell Biology, University of Western Ontario for training in the use of the Amira software.

NOTES ON CONTRIBUTORS

JEREMY A. ROTH, M.Sc., is a senior anatomy demonstrator in the School of Anatomy, Department of Kinesiology at the University of Waterloo, Waterloo, Canada. He received his M.Sc. degree in clinical anatomy from the Department of Anatomy and Cell Biology at Western University, London, Ontario, Canada. The research presented in this report was part of his M.Sc. project.

TIMOTHY D. WILSON, Ph.D., is an associate professor in the Department of Anatomy and Cell Biology at Western University, London, Ontario, Canada. He is the director of the Corps for Research of Instructional and Perceptual Technologies (CRIPT) laboratory investigating digital anatomy. He teaches gross anatomy at a variety of graduate and undergraduate levels.

MARTIN SANDIG, Ph.D., is an associate professor in the Department of Anatomy and Cell Biology at Western University, London, Ontario, Canada. He is a member of the Corps for Research of Instructional and Perceptual Technologies (CRIPT) laboratory investigating digital anatomy. He teaches histology and cell biology at a variety of graduate and undergraduate levels.

LITERATURE CITED

Adams CM, Wilson TD. 2011. Virtual cerebral ventricular system: An MR-based three-dimensional computer model. Anat Sci Educ 4:340–347.

Allen LK, Bhattachcharyya S, Wilson TD. 2015. Development of an interactive anatomical eye model. Anat Sci Educ 8:275–282.

Barbeau ML, Johnson M, Gibson C, Rogers KA. 2013. The development and assessment of an online microscopic anatomy laboratory course. Anat Sci Educ 6:246–256.

Blumer MJ, Gahleitner P, Narzt T, Handl C, Ruthensteiner B. 2002. Ribbons of semithin sections: An advanced method with a new type of diamond knife. J Neurosci Methods 120:11–16.

Braun MW, Kearns KD. 2008. Improved learning efficiency and increased student collaboration through use of virtual microscopy in the teaching of human pathology. Anat Sci Educ 1:240–246.

Cho CR, Winslow J, Whiteside C, Lumsden CJ. 1991. A new computer-assisted three-dimensional reconstruction method provides accurate measurement of glomerular mesangial volume. J Electron Microsc Tech 18:249–261.

Christensen EI, Grann B, Kristoffersen IB, Skriver E, Thomsen JS, Andreasen A. 2014. Three-dimensional reconstruction of the rat nephron. Am J Physiol Renal Physiol 306:F664–F671.

Chung K, Wallace J, Kim SY, Kalyanasundaram S, Andalman AS, Davidson TJ, Mirzabekov JJ, Zalocusky KA, Mattis J, Denisin AK, Pak S, Bernstein H, Ramakrishnan C, Grosenick L, Gradinaru V, Deisseroth K. 2013. Structural and molecular interrogation of intact biological systems. Nature 497:332–337.

Codd AM, Choudhury B. 2011. Virtual reality anatomy: Is it comparable with traditional methods in the teaching of human forearm musculoskeletal anatomy? Anat Sci Educ 4:119–125.

Collier L, Dunham S, Braun MW, O'Loughlin VD. 2012. Optical versus virtual: Teaching assistant perceptions of the use of virtual microscopy in an undergraduate human anatomy course. Anat Sci Educ 5:10–19.

CRIPT. 2015. Corps for Research of Instructional and Perceptual Technologies. 3D Renal Corpuscle from Histological Sections. Schulich School of Medicine and Dentistry, Western University, London, Ontario, Canada. URL: http://www.anatatorium.com/CRIPT/Renal_Corpuscle.html [accessed 17 February 2015].

D'Amico F. 2005. A polychromatic staining method for epoxy embedded tissue: A new combination of methylene blue and basic fuchsine for light microscopy. Biotech Histochem 80:207–210.

Drake RL, McBride JM, Lachman N, Pawlina W. 2009. Medical education in the anatomical sciences: The winds of change continue to blow. Anat Sci Educ 2:253–259.

Elizondo-Omaña RE, Morales-Gómez JA, Guzmán SL, Hernández IL, Ibarra RP, Vilchez FC. 2004. Traditional teaching supported by computer-assisted learning for macroscopic anatomy. Anat Rec 278B:18–22.

Estevez ME, Lindgren KA, Bergethon PR. 2010. A novel three-dimensional tool for teaching human neuroanatomy. Anat Sci Educ 3:309–317.

Goldberg HR, Dintzis R. 2007. The positive impact of team-based virtual microscopy on student learning in physiology and histology. Adv Physiol Educ 31:261–265.

Hallgren RC, Parkhurst PE, Monson CL, Crewe NM. 2002. An interactive, web-based tool for learning anatomic landmarks. Acad Med 77:263–265.

Handschuh S, Schwaha T, Metscher BD. 2010. Showing their true colors: A practical approach to volume rendering from serial sections. BMC Dev Biol 10:41

Harris T, Leaven T, Heidger P, Kreiter C, Duncan J, Dick F. 2001. Comparison of a virtual microscope laboratory to a regular microscope laboratory for teaching histology. Anat Rec 265:10–14.

Helle L, Nivala M, Kronqvist P. 2013. More technology, better learning resources, better learning? Lessons from adopting virtual microscopy in undergraduate medical education. Anat Sci Educ 6:73–80.

Henry EC. 1977. A method for obtaining ribbons of serial sections of plastic embedded specimens. Stain Technol 52:59–60.

Higazi TB. 2011. Use of interactive live digital imaging to enhance histology learning in introductory level anatomy and physiology classes. Anat Sci Educ 4:78–83.

Hu A, Wilson T, Ladak H, Haase P, Fung K. 2009. Three-dimensional educational computer model of the larynx: Voicing a new direction. Arch Otolaryngol Head Neck Surg 135:677–681.

Husmann PR, O'Loughlin VD, Braun MW. 2009. Quantitative and qualitative changes in teaching histology by means of virtual microscopy in an introductory course in human anatomy. Anat Sci Educ 2:218–226.

Inkyo-Hayasaka K, Sakai T, Kobayashi N, Shirato I, Tomino Y. 1996. Three-dimensional analysis of the whole mesangium in the rat. Kidney Int 50:672–683.

Karnovsky MJ. 1965. A formaldehyde-glutaraldehyde fixative of high osmolarity for use in electron microscopy. J Cell Biol 27:137A.

Keedy AW, Durack JC, Sandhu P, Chen EM, O'Sullivan PS, Breiman RS. 2011. Comparison of traditional methods with 3D computer models in the instruction of hepatobiliary anatomy. Anat Sci Educ 4:84–91.

Martin CM, Roach VA, Nguyen N, Rice CL, Wilson TD. 2013. Comparison of 3D reconstructive technologies used for morphometric research and the translation of knowledge using a decision matrix. Anat Sci Educ 6:393–403.

Metzler R, Stein D, Tetzlaff R, Bruckner T, Meinzer HP, Buchler MW, Kadmon M, Muller-Stich BP, Fischer L. 2012. Teaching on three-dimensional presentation does not improve the understanding of according CT images: A randomized controlled study. Teach Learn Med 24:140–148.

Mollenhauer HH. 1964. Plastic embedding mixtures for use in electron microscopy. Stain Technol 39:111–114.

Neal CR, Crook H, Bell E, Harper SJ, Bates DO. 2005. Three-dimensional reconstruction of glomeruli by electron microscopy reveals a distinct restrictive urinary subpodocyte space. J Am Soc Nephrol 16:1223–1235.

Nguyen N, Wilson TD. 2009. A head in virtual reality: Development of a dynamic head and neck model. Anat Sci Educ 2:294–301.

Nicholson DT, Chalk C, Funnell WR, Daniel SJ. 2006. Can virtual reality improve anatomy education? a randomised controlled study of a computer-generated three-dimensional anatomical ear model. Med Educ 40:1081–1087.

Petersson H, Sinkvist D, Wang C, Smedby O. 2009. Web-based interactive 3D visualization as a tool for improved anatomy learning. Anat Sci Educ 2:61–68.

Pinder KE, Ford JC, Ovalle WK. 2008. A new paradigm for teaching histology laboratories in canada's first distributed medical school. Anat Sci Educ 1: 95–101.

Qayumi AK, Kurihara Y, Imai M, Pachev G, Seo H, Hoshino Y, Cheifetz R, Matsuura K, Momoi M, Saleem M, Lara-Guerra H, Miki Y, Kariya Y. 2004. Comparison of computer-assisted instruction (CAI) versus traditional textbook methods for training in abdominal examination (Japanese experience). Med Educ 38:1080–1088.

Remuzzi A, Brenner BM, Pata V, Tebaldi G, Mariano R, Belloro A, Remuzzi G. 1992. Three-dimensional reconstructed glomerular capillary network: Blood flow distribution and local filtration. Am J Physiol 263:F562–F572.

Ruisoto P, Juanes JA, Contador I, Mayoral P, Prats-Galino A. 2012. Experimental evidence for improved neuroimaging interpretation using three-dimensional graphic models. Anat Sci Educ 5:132–137.

Ruthensteiner B. 2008. Soft part 3D visualization by serial sectioning and computer reconstruction. In: Geiger DL, Ruthensteiner B (Editors). Micromolluscs: Methodological Challenges—Exciting Results Methodological. Proceedings from the Micromollusc Symposium of the 16th UNITAS Malacologica World Congress of Malacology, July 15–20, 2007 in Antwerp, Belgium. 1st Ed. Auckland, New Zealand: Magnolia Press. p 63–100.

Ruthensteiner B, Baeumler N, Barnes DG. 2010. Interactive 3D volume rendering in biomedical publications. Micron 41:886.e1–886.e17.

Sergovich A, Johnson M, Wilson TD. 2010. Explorable three-dimensional digital model of the female pelvis, pelvic contents, and perineum for anatomical education. Anat Sci Educ 3:127–133.

Silén C, Wirell S, Kvist J, Nylander E, Smedby O. 2008. Advanced 3D visualization in student-centred medical education. Med Teach 30:e115–e124.

Tam MD. 2010. Building virtual models by postprocessing radiology images: A guide for anatomy faculty. Anat Sci Educ 3:261–266.

Trelease RB, Rosset A. 2008. Transforming clinical imaging data for virtual reality learning objects. Anat Sci Educ 1:50–55.

Venail F, Deveze A, Lallemant B, Guevara N, Mondain M. 2010. Enhancement of temporal bone anatomy learning with computer 3D rendered imaging software. Med Teach 32:e282–e288.

Ware RW. 1975. Three-dimensional reconstruction from serial sections. Int Rev Cytol 40:325–440.

Wilson TD. 2015. Role of image and cognitive load in anatomical multimedia. In: Chan LK, Pawlina W (Editors). Teaching Anatomy: A Practical Guide. 1st Ed. New York, NY: Springer International Publishing. p 237–246.

Yeung JC, Fung K, Wilson TD. 2011. Development of a computer-assisted cranial nerve simulation from the visible human dataset. Anat Sci Educ 4:92–97.

Zhai XY, Thomsen JS, Birn H, Kristoffersen IB, Andreasen A, Christensen EI. 2006. Three-dimensional reconstruction of the mouse nephron. J Am Soc Nephrol 17:77–88.